

Crystallization from the Glassy State

JOHN R. COLLIER* and ERIC BAER, *Polymeric Science and Engineering, Case Institute of Technology, Cleveland, Ohio*

Synopsis

Isothermal crystallization of poly[3,3-bis(chloromethyl)oxacyclobutane] and poly(ethylene terephthalate) from the quenched glassy state gave small lamellae approximately 1000-2000 Å. in lateral dimension with a constant thickness of about 100 Å. The maximum primary nuclei density for crystallization slightly above the glass transition temperature, T_g , was 10^{10} greater than frequently observed during spherulitic growth from the melt. Since the lamellae grow at a linear rate, the crystallization process could be described by the Avrami theory for two-dimensional growth with a constant nuclei density. By assuming that crystallization near T_g is diffusion-controlled, bulk crystallization rate data were analyzed to obtain self-diffusion coefficients whose activation energies were similar to reported values for other polymers.

INTRODUCTION

Crystallization from the glassy state at temperatures considerably above the glass transition temperature, T_g , has been shown to result in spherulitic growth.¹⁻³ Between T_g and the temperature at which spherulites are readily observable, polymers have been postulated to exist in a transcrystalline state.⁴ Also a pseudo-structure^{5,6} with difficult-to-resolve fibrous structures has been suggested.^{1,7} However, small-angle x-ray long-period spacings of about 100 Å. have been repeatedly observed in polymers crystallized in this temperature region.^{3,5,6,8,9}

Dilatometric measurements of bulk crystallization rates from the glass were observed to fit the Avrami theory¹⁰⁻¹² and exhibited significant differences to crystallization from the melt, suggesting a different crystallization mechanism.^{13,14} Near the melting temperature the crystallization rate is controlled by the surface nucleation rate, and near the glass transition by the self-diffusion of molecular segments to the growing crystal surface, thereby, giving rise to a maximum in the crystallization rate at an intermediate temperature.¹⁵⁻¹⁸

The self-diffusion of polymer segments has been studied by placing a thin layer of radioactive polymer on a plane block of a similar, but nonradioactive, polymer and measuring the decrease of radioactivity of the upper surface as a function of time.^{19,20} From these studies and other theoretical considerations it has been postulated that polymer chains migrate through the bulk polymer in kinetic units of approximately 20 to 40 carbon

* Present address: Department of Chemical Engineering, Ohio University, Athens, Ohio.

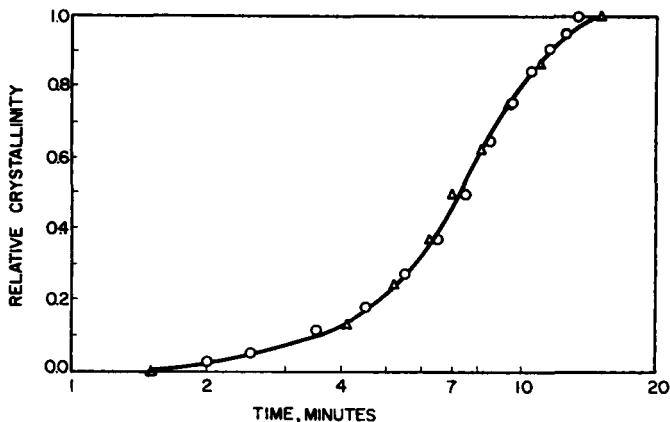


Fig. 1. Agreement between corrected (O) photometric and (Δ) dilatometric crystallization curves for polypropylene at 125°C.

atoms in length and that the activation energy for this process is the same order of magnitude as the activation energy for viscous flow.^{19,21,23}

In this paper the morphology, the crystallization kinetics, and the self-diffusion phenomenon in two polymers crystallized from the glassy state are discussed.

EXPERIMENTAL

The samples used in this investigation were extruded pellets of poly-[3,3-bis(chloromethyl)oxacyclobutane], Penton,* and 2-mil poly(ethylene terephthalate) (PET) which were generously supplied by the Hercules Powder Company and E. I. Du Pont de Nemours and Co., respectively. Using a platen press the Penton pellets were molded into a film 1 mm. thick and then cooled from the melt by circulating cooling water through the platens. Circular disks, $\frac{3}{4}$ in. in diameter, were punched out of these films and sandwiched between two steel disks of the same diameter. Each metal disk had a $\frac{1}{8}$ -in. diameter hole in its center, which enabled crystallization to occur in a free surface region. Unless otherwise specified in the text, the Penton samples were maintained at 230°C. for 1 hr. and the PET samples at 300°C. for 5 min. prior to quenching to the glassy amorphous state in ice water.

These samples were allowed to crystallize above their T_g in an air circulation chamber which maintained temperatures up to 250°C. with fluctuations of less than $\pm 0.05^\circ\text{C}$.¹⁵ The crystallization process was observed through a polarizing microscope equipped with long working distance objectives, and the extent of crystallization was measured with a photocell, the output being recorded on a Sargent SR recorder.

The basic principle of deriving a crystallization curve from photometric data is that a relative change of crystallinity causes a corresponding relative change in the diffracted polarized light intensity.^{24,25} The photocell re-

* Registered trademark of the Hercules Powder Co.

sponse which is directly proportional to the incident light intensity change raised to a power, was calibrated experimentally by using dilatometric data.^{26,27} In Figure 1, good agreement between corrected (raised to a power of 1.2) photometric²⁷ and dilatometric crystallization²⁸ curves is shown for polypropylene crystallized at 125°C. from the melt.

RESULTS AND DISCUSSION

Morphology

Electron micrographs of free and fracture surfaces of Penton crystallized isothermally from the glass showed lamellar structures with irregular boundaries. A typical example given in Figure 2 shows random structures which on the average are 75 Å. thick and have lateral dimensions ranging between 1000 and 2000 Å. No interconnections which are common in axiallites, dendrites, and spherulites²⁹ were observed, and cleavage at liquid nitrogen temperatures showed no evidence of drawing. Since the lamellae in glass-crystallized samples are oriented randomly, it was possible to measure their thickness both from lamellae which were perpendicular to the free surface (*B*) and from the replica shadows of lamellae parallel to the surface (*A*). As expected, measured thicknesses of both parallel and perpendicular lamellae agreed within experimental error. Due to the small

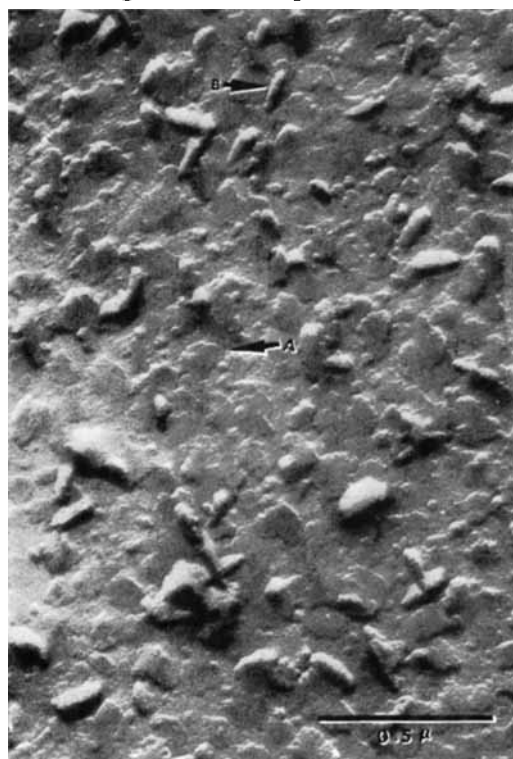


Fig. 2. Electron micrograph of Penton free surface sample crystallized from the glass at 33.4°C. Magnification 73,900 \times .

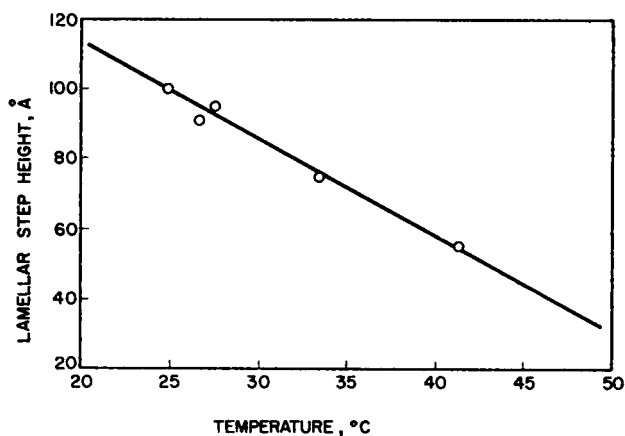


Fig. 3. Variation of lamellar thickness with crystallization temperature for Penton.

size of the lamellae, no observable structure could be detected by use of an optical microscope. However, when viewed through crossed polarizers during crystallization, the field of observation became brighter as time progressed.

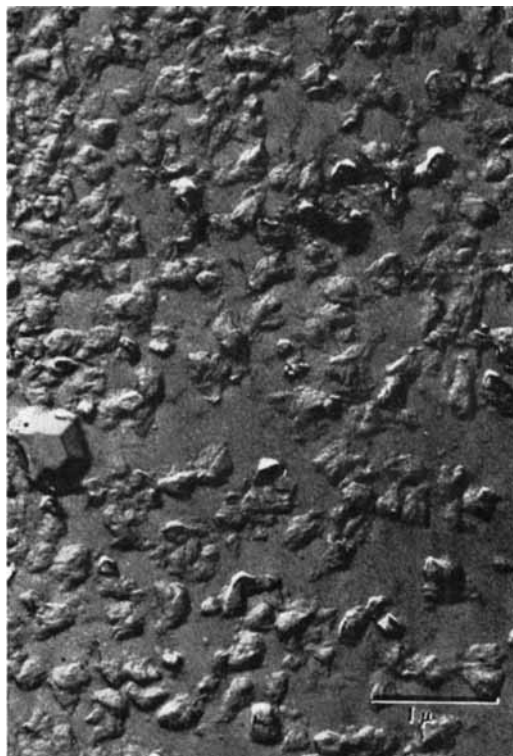


Fig. 4. Electron micrograph of PET free surface crystallized from the glass at 97.0°C. Magnification 25,500 \times .

The effect of crystallization temperature on lamellar thickness is shown in Figure 3. A substantial decrease from 100 Å. at 24.9°C. to 55 Å. at 41.2°C. was observed. This dependence upon the temperature differential above T_g is similar to the effect of temperature differential on the lamellar thickness observed during crystallization from the melt. In both cases an increasing temperature differential increases the crystallization rate and decreases the lamellar thickness.

Figure 4 illustrates that similar lamellae appear when PET is crystallized from the glass at 97.0°C. However, these lamellae are not as flat in appearance as in Penton. This may be related to the difficulty encountered in attempts to grow PET single crystals from solution.³⁰ The highly ordered hexagonal bipyramids which were also observed are similar in appearance to structures noted by other investigators who identified them as low molecular weight polyester.^{31,32}

When the free surface technique was not used prior to quenching and crystallization, impressions of the constraining medium remained after crystallization making it difficult to resolve any morphological structure. It is possible that due to this surface-impression effect Mayhan et al.³³ did not observe lamellar structure following the crystallization of amorphous cast films from the glass.

Nucleation

The maximum nuclei density in glass-crystallized samples was estimated by counting the number of lamellae per unit surface area and found to be about 10^{10} nuclei/cm.² in both polymers. Dividing by the lamellar thickness, the maximum nuclei density is calculated to be 10^{16} nuclei/cm.³. It is interesting to compare this large value with the primary nuclei density for spherulitic crystallization from the melt which was measured to be about 10^6 nuclei/cm.³ in Penton. The fact that nearly all of the lamellae in Figure 2 appear to be approximately the same size indicates that a constant nuclei density must have occurred during most of the crystallization process. The appearance of nuclei was probably a function of time only during a short initial period.

Crystallization Kinetics

The crystallization kinetics in thin films was studied by using a photometric technique which gave relative crystallinity as a function of time. Typical sigmoidal crystallization curves for Penton and PET are shown in Figures 5 and 6 to be strongly dependent upon the temperature differential above their respective glass transition temperatures. The observed crystallization half-times, $\tau_{1/2}$, and data from additional isothermal measurements are summarized in Tables I and II.

Several investigators have suggested that near the melting point surface nucleation governs the crystallization kinetics, whereas near the glass transition molecular diffusion is the controlling mechanism.¹⁵⁻¹⁷ Consider a lamellar crystal of thickness l growing outward from the nucleus.

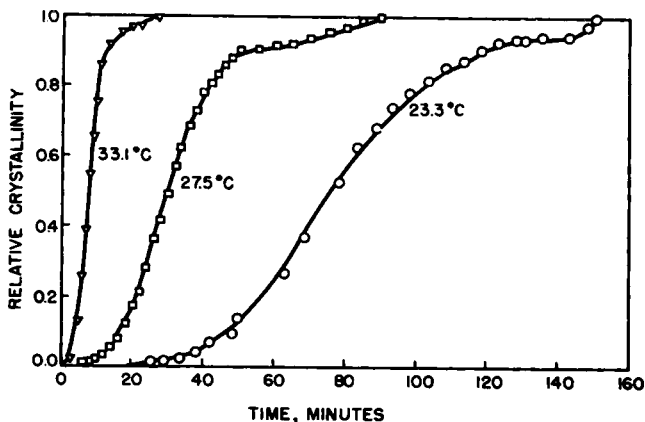


Fig. 5. Selected Penton isothermal crystallization rate curves.

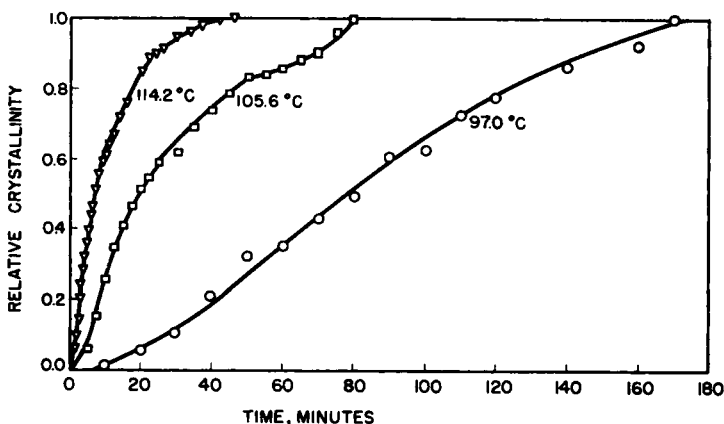


Fig. 6. Selected PET isothermal crystallization rate curves.

For simplicity, the crystal was assumed to be circular with radius r , although in reality the crystal assumes a polyhedral shape. If the radial growth is controlled by segmental chain diffusion to the crystal, the lateral surface area A increases as a linear function of time t , that is,

$$A = Dt \quad (1)$$

where D is the self-diffusion coefficient. Since the lamellar crystal has a constant thickness, $A = 2\pi r l$, and substitution into eq. (1) gives

$$r = (D/2\pi l) t \quad (2)$$

Equation (2) predicts a linear growth rate for the lamellar crystals, suggesting that the Avrami theory can readily be applied.³⁴⁻³⁷ The amorphous fraction, ϕ , as a function of time is

$$\ln \phi = -Kt^n \quad (3)$$

where K and n are constants determined by the dimensionality of growth and the nucleation characteristics. Since lamellar growth is essentially two-dimensional, and a constant nuclei density exists during most of the

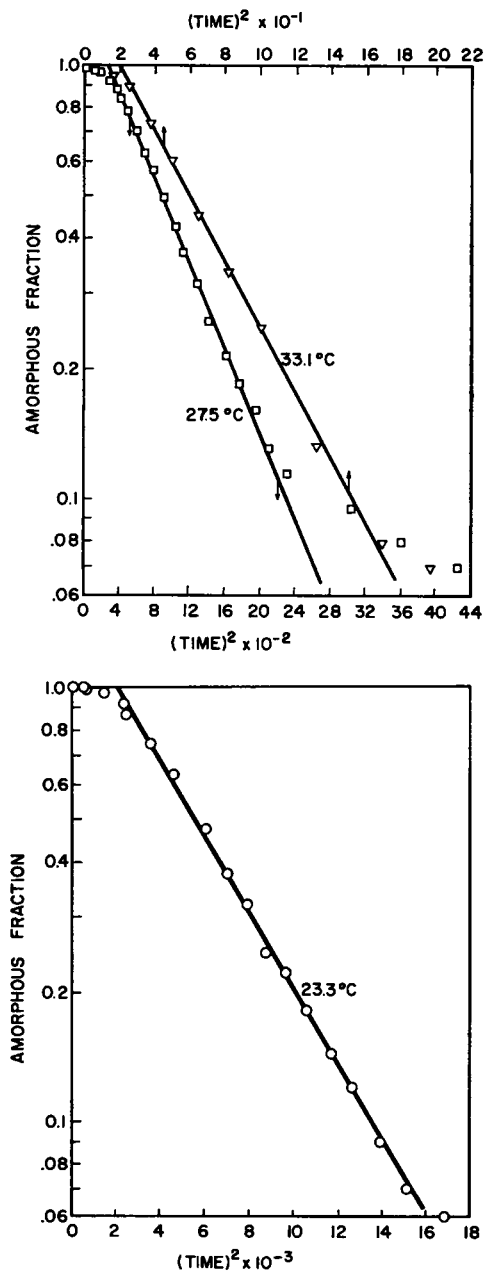


Fig. 7. Avrami fit of selected Penton isothermal crystallization rate curves.

TABLE I
 Self-Diffusion Data for Penton^a

Crystallization temperature, °C.	Crystallization half-time $\tau_{1/2}$, min.	Lamellar thickness, A.	Diffusion coefficient $D \times 10^{14}$, cm. ² /sec.
23.3	50	100	1.0
24.9	38	100	1.3
26.6	28	95	1.6
27.5	24	93	1.9
30.6	9.2	84	4.5
33.1	6.5	77	5.8
33.4	3.8	76	9.8
41.2	1.7	55	34

^a Nuclei density assumed constant and equal to 10^{10} nuclei/cm.².

 TABLE II
 Self-Diffusion Data For PET^a

Crystallization, °C.	Crystallization $\tau_{1/2}$, min.	Diffusion coefficient $D \times 10^{14}$, cm. ² /sec.
84.9	1,700	0.029
93.6	90	0.55
97.0	76	0.65
102.4	35	1.4
105.6	20	2.5
106.2	15	3.3
107.2	10	4.9
114.2	6.0	82

^a Nuclei density and lamellar step are assumed constant and equal to 10^{10} nuclei/cm.² and 100 A., respectively.

crystallization process, n should be equal to 2. Also, it can be readily shown that

$$K = \rho_n D^2 / 4\pi l^2 \quad (4)$$

where ρ_n is the number of nuclei per unit area.

The bulk crystallization data presented in Figure 5 are replotted in Figures 7a and 7b according to the Avrami theory. Good agreement is obtained between 10 and 90% relative crystallinities. The discrepancies noted at low crystallinities are probably due to the formation with the time of new nuclei, while disagreement with theory near the end of the crystallization process could be caused by the lamellar growth becoming nonlinear due to segregation of impurities, as suggested by Keith and Padden.³⁸

The coefficient of self-diffusion can readily be calculated by combining eqs. (3) and (4) which gives

$$D = (2l/\tau_{1/2})[-\pi \ln (1/2)/\rho_n]^{1/2} \quad (5)$$

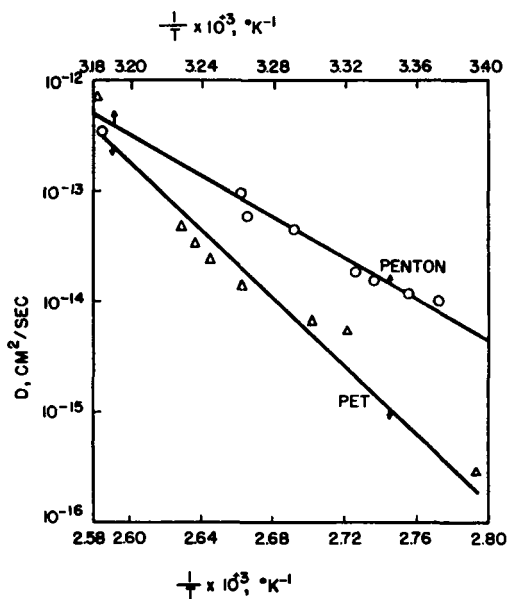


Fig. 8. Temperature dependence of Penton and PET diffusion coefficients.

when using the crystallization half time, $\tau_{1/2}$. In tables I and II, the self-diffusion coefficients calculated by using eq. (5) are given as a function of the crystallization temperatures. As expected, these coefficients are of the same order of magnitude as those reported for other polymers using independent techniques.³⁹

Various authors^{20,39,40} have shown that the temperature dependence of D follows an Arrhenius relationship

$$D = D_0 \exp\{E_D/RT\} \quad (6)$$

where E_D is the activation energy for self diffusion which is postulated to be approximately equal to the activation energy for viscous flow.³⁹ A plot of $\log D$ versus the reciprocal temperatures is shown in Figure 8 for both polymers. The activation energies were found to be 38 and 64 kcal./mole of repeat unit for Penton and PET, respectively. Although these activation energies are on the same order of magnitude as those reported for other polymers using different detection techniques,³⁹ the PET value is slightly higher than previous reported values which range up to 50 kcal./mole of repeat unit.⁴¹ Since the activation energies of self-diffusion have been determined for very few polymers, a more valid comparison may be reported activation energies for viscous flow. Values ranging up to 70 kcal./mole of repeat unit for cellulose acetate⁴⁰ have been reported. PET has a high cohesive energy density⁴² and would be expected to have a high activation energy because of its helical rather rigid chain and the polar groups.³⁹

CONCLUSIONS

Isothermal crystallization from the glassy state in both Penton and PET gave small lamellar crystals about 100 Å thick and between 1000 and 2000 Å in lateral dimension. The maximum nuclei density in glass-crystallized material was estimated to be 10^{16} nuclei/cm.³, which is considerably larger than 10^6 nuclei/cm.³ found for samples crystallized from the melt.

Bulk crystallization rate data obtained at various temperatures above T_g were analyzed by using the Avrami theory for two-dimensional growth assuming a constant nuclei density throughout most of the crystallization process. By using measured values for the lamellar thickness, the nuclei density and the crystallization half time, the coefficient for self-diffusion was calculated as a function of crystallization temperature. Activation energies for self-diffusion calculated assuming an Arrhenius type relationship were in reasonable agreement with previously reported values.

The authors gratefully acknowledge the generous financial assistance of the National Aeronautic and Space Administration, and are indebted to Dr. C. E. Rogers for stimulating discussions and suggestions.

References

1. J. Majer, *Kunststoffe*, **55**, 11 (1965).
2. G. Kampf, *Kolloid-Z.*, **172**, 50 (1960).
3. R. Eppe, E. W. Fischer, and H. A. Stuart, paper presented at International High Polymer Conference, Nottingham, July 21–24, 1958.
4. E. Jenckel, E. Teege, and W. Hinrichs, *Kolloid-Z.*, **129**, 19 (1952).
5. H. G. Kilian, H. Halboth, and E. Jenckel, *Kolloid-Z.*, **172**, 166 (1960).
6. K. H. Illers and H. Breuer, *J. Colloid Sci.*, **18**, 1 (1963).
7. D. J. H. Sandiford, *J. Appl. Chem.*, **8**, 188 (1958).
8. H. G. Kilian, *Kolloid-Z.*, **176**, 49 (1961).
9. H. A. Stuart, *Kolloid-Z.*, **165**, 3 (1959).
10. F. D. Hartley, F. W. Lord, and L. B. Morgan, *Phil. Trans.*, **A247**, 23 (1954).
11. W. H. Cobbs and R. L. Burton, *J. Polymer Sci.*, **10**, 275 (1953).
12. R. C. Golike and W. H. Cobbs, Jr., *J. Polymer Sci.*, **54**, 277 (1964).
13. L. B. Morgan, *J. Appl. Chem.*, **4**, 160 (1954).
14. A. Keller, G. D. Lester, and L. B. Morgan, *Phil. Trans.*, **A247**, 1 (1954).
15. E. Baer, J. R. Collier, and D. R. Carter, *SPE Trans.*, **5**, 22 (1965).
16. B. B. Burnett and W. F. McDevitt, *J. Appl. Phys.*, **88**, 1101 (1957).
17. W. J. Barnes, W. G. Luetzel, and F. P. Price, *J. Phys. Chem.*, **65**, 1742 (1961).
18. M. Takayanagi, *Mem. Fac. Eng. Kyushu Univ.*, **16**, 111 (1957).
19. S. S. Voyutskii, *Autohesion and Adhesion of High Polymers*, Interscience, New York, 1963.
20. D. W. McCall, D. C. Douglass, and E. W. Anderson, *J. Chem. Phys.*, **30**, 771 (1959).
21. G. M. Pavlyucheuko, T. V. Gatovskaya, and V. A. Kartin, *Rubber Chem. Technol.*, **36**, 1003 (1963).
22. H. Eyring and W. Kauzmann, *J. Am. Chem. Soc.*, **62**, 3113 (1940).
23. P. J. Flory, *J. Am. Chem. Soc.*, **62**, 1057, 3032 (1940).
24. J. H. Magill, *Nature*, **191**, 1092 (1961).
25. C. W. Bunn, *Fibers From Synthetic Polymers*, R. Hill, Ed., Elsevier, Amsterdam, 1953.
26. Clairex Photoconductive Cells Technical Bulletin.
27. J. R. Collier, Ph.D. Thesis, Case Institute of Technology, 1966.

28. L. Marker, P. M. Hay, G. P. Tilley, R. M. Early, and O. J. Sweeting, *J. Polymer Sci.*, **38**, 33 (1959).
29. H. D. Keith, *J. Polymer Sci. A*, **2**, 4339 (1964).
30. G. Yeh, personal communication.
31. R. Giuffria, *J. Polymer Sci.*, **49**, 427 (1961).
32. Yu. Ya. Tonpaskpol'skiĭ, A. Zubov, and G. S. Markiva, *Vysokomolekul. Soedin.*, **6**, 154 (1964).
33. K. G. Mayhan, W. J. James, and W. Bosch, *J. Appl. Polymer Sci.*, **9**, 3617 (1965).
34. M. Avrami, *J. Chem. Phys.*, **7**, 1103 (1939).
35. U. R. Evans, *Trans. Faraday Soc.*, **41**, 365 (1945).
36. M. Avrami, *J. Chem. Phys.*, **8**, 212 (1940).
37. M. Avrami, *J. Chem. Phys.*, **9**, 177 (1941).
38. H. D. Keith and F. J. Padden, Jr., *J. Appl. Phys.*, **35**, 1286 (1964).
39. S. S. Voyutskii and V. L. Vakula, *Rubber Chem. Technol.*, **37**, 1153 (1964).
40. F. Bueche, W. M. Cashin, and P. Debye, *J. Chem. Phys.*, **20**, 1956 (1952).
41. R. P. Kambour and F. L. Pilar, *Am. Chem. Soc. Preprint, Div. Polymer Chem.*, **2**, No. 2, 175 (1961).
42. E. C. Bernhart *Processing of Thermoplastic Materials*, Reinhold, New York, 1959.
43. F. W. Billmeyer, Jr., *Textbook of Polymer Science*, Interscience, New York, 1962.

Résumé

La cristallisation isotherme du poly[3,3-bis(chlorométhyl)oxacyclobutane] et du téréphtalate de polyéthylène au départ de l'état vitreux refroidi fournit de petites lamelles approximativement de 1.000 à 2.000 Å. de dimension latérale, avec une épaisseur constante d'environ 100 Å. La densité maximum de noyaux primaires pour une cristallisation légèrement au-dessus de la température de transition vitreuse T_g est 10^{10} fois plus grande que celle observée au cours de la croissance sphérolitique au départ de la masse fondue. Comme ces lamelles croissent à une vitesse linéaire, le processus de cristallisation peut être décrit par la théorie d'Avrami pour une croissance bidimensionnelle avec une densité de noyaux constante. En admettant que la cristallisation au voisinage de T_g est contrôlée par la diffusion, la vitesse de cristallisation en masse fournit des résultats qui ont été analysés en vue d'obtenir des coefficients de diffusion dont l'énergie d'activation était semblable aux valeurs reportées pour les autres polymères.

Zusammenfassung

Die isotherme Kristallisation von Poly[3,3-bis(chlormethyl)oxacyclobutan] und Polyäthylenterephtalat aus dem abgeschreckten Glaszustand lieferte kleine Lamellen mit einer seitlichen Dimension von etwa 1000 bis 2000 Å und einer konstanten Dicke von etwa 100 Å. Die grösste Dichte an Primärkeimen war bei einer Kristallisation schwach oberhalb der Glasumwandlungstemperatur T_g 10^{10} mal grösser als die häufig beim Sphärolithwachstum aus der Schmelze beobachtete. Da die Lamellen mit linearer Geschwindigkeit wachsen, konnte der Kristallisationsprozess mit der Avrami-Theorie für zweidimensionales Wachstum mit konstanter Keimdichte erfasst werden. Unter der Annahme, dass die Kristallisation in der Nähe von T_g diffusionskontrolliert ist, wurden die Kristallisationsgeschwindigkeitsdaten zur Gewinnung von Selbstdiffusionskoeffizienten ausgewertet, deren Aktivierungsenergie sich den bekannten Werten für andere Polymere als ähnlich erwies.

Received March 16, 1966
Prod. No. 1370